ELSEVIER

Microelectronics Journal 34 (2003) 695–699

Microelectronics Journal

www.elsevier.com/locate/mejo

Hybrid and effective satellites for studying superlattices

S.L. Morelhão[a,*], A.A. Quivy[a], J. Härtwig[b]

[a]*Instituto de Física, USP, CP 66318, 05315-970 São Paulo, SP, Brazil*
[b]*European Synchrotron Radiation Facility, BP 220, F-38043 Grenoble, France*

Abstract

Observation of new synchrotron X-ray scattering processes in semiconductor superlattice structures are reported. They are analogous to the three-beam diffraction in single crystal; however, the basic difference is that in these new processes superlattice-satellite reflections came to play. They give rise to effective-satellite reflections (superlattice–superlattice coupling) and hybrid-satellite reflections (substrate–superlattice coupling). These sort of reflections are features that depend on the rotation of the sample around the surface-normal direction, i.e. an azimuthal or ϕ rotation. Their positions in ϕ are very sensitive to the in-plane projection of the reciprocal space, but while the effective-satellite reflections are sensitive to the superlattice parameters, the positions of the hybrid-satellite reflections depend mostly on the substrate ones. The selective sensitivity of these two sort of reflections is the physical fact that can be used as a new tool for studying superlattices.

PACS: 61.10.Nz; 61.72.Dd; 81.05.Ea

Keywords: Three-beam X-ray diffraction; Synchrotron radiation; Superlattice; Satellite reflections; Semiconductors

1. Introduction

In the research and development of semiconductor devices for micro- and optoeletronic applications, X-ray diffraction is a very important non-destructive characterization tool. Double-crystal rocking curves and reciprocal space mapping are standard and powerful high-resolution diffraction techniques for analyzing semiconductor epitaxial structures. These techniques investigate the X-ray scattering by the sample on a two-beam diffraction (2-BD) geometry, which imply that all features relevant to diffraction physics are described in the plane of incidence—the plane defined by the incident and diffracted beams. Consequently, in the commercially available ready-to-use diffractometers for high-resolution diffraction, the X-ray beam is mostly conditioned in the plane of incidence. Recently, in searching of alternative methods for analyzing semiconductor devices on high-resolution diffractometers, the reciprocal space around a particular 3-BD of the substrate lattice has been investigated [1]. The reciprocal space analysis of that particular case have shown experimentally a stronger wavefield attenuation in depth than for the same Bragg reflection alone. The investigation was also extended to the study of superlattices, where some of the results have suggested the occurrence of a new scattering process named effective satellites. Since in standard high-resolution X-ray diffractometers the incident beam is not conditioned perpendicularly to the plane of incidence, further investigation on effective satellites had to be carried out synchrotron facilities.

Here we report the accomplishment of two-dimensional intensity mapping around 3-and 6-BDs on semiconductor superlattice structures with synchrotron X-rays. The results confirm that theoretical approaches for describing effective satellites are correct as well as the hypothesis on hybrid satellites. Besides the experimental results themselves, discussion and characterization, this work also brings mathematical developments for greatly improving the understanding and applicability of the observed phenomenon.

2. Basic theory

3-BD arises when an incident monochromatic beam simultaneously satisfies the Bragg law for two reflections within a crystal. In most case, it is generated when the crystal is first aligned by a ω rotation—the rocking angle—for a symmetric Bragg reflection, the primary reflection P. The ϕ rotation—the azimuthal angle—of

* Corresponding author. Tel.: +55-11-818-7012; fax: +55-11-818-6749.
E-mail address: morelhao@if.ups.br (S.L. Morelhão).

0026-2692/03/$ - see front matter © 2003 Elsevier Science Ltd. All rights reserved.
doi:10.1016/S0026-2692(03)00101-0

the crystal around the diffraction vector of the primary reflection, **P**, brings another reflection, the secondary reflection ***S***, to diffract simultaneously. The primary and secondary beam directions are given by the wavevectors $\mathbf{k}_P = \mathbf{P} + \mathbf{k}_0$ and $\mathbf{k}_S = \mathbf{S} + \mathbf{k}_0$, respectively, where $\mathbf{k}_0$ is the wave-vector of the incident beam. Although, there is symmetry in the energy balance from one beam to another, we will concern here only with the extra amount of intensity transferred from the secondary beam to the primary one. The coupling reflection ***C*** is responsible for such a transfer since $\mathbf{k}_P$ is also given by $\mathbf{k}_P = \mathbf{C} + \mathbf{k}_S$. In terms of the incident beam direction, it can be expressed as $\mathbf{k}_P = \mathbf{C} + \mathbf{S} + \mathbf{k}_0$, or $\mathbf{k}_P = \mathbf{P}^* + \mathbf{k}_0$ where $\mathbf{P}^* = \mathbf{C} + \mathbf{S}$ is the reciprocal vector of the effective primary reflection, also known as detour reflection. Hereafter, the superscript $*$ is used to specify *effective* diffraction peaks.

Superlattices are heteroepitaxial structures grown on top of single crystal substrates and made of a repetition of an identical sub-structure of epilayers—the base epilayers. Their large periodicity, ***D***, in real space gives rise to several satellite reflections that are visible due to the X-ray scattering by the reflections of the crystalline lattice in the epilayers of the base. With respect to the substrate reciprocal vectors, **G**, the satellites are located in the reciprocal space by vectors such as $\mathbf{G}^{(n)} = \mathbf{G} + (\Delta q_G + n/D)\hat{z}$, where $\hat{z}$ is the surface-normal direction, n the satellite index, 0, ± 1, ± 2,..., and Δq_G is the distance of the zeroth-order satellite (SL0, $n = 0$) from $\mathbf{G}\cdot\hat{z}$, the normal component of **G**.

3. Theory of effective and hybrid satellites

Besides the expected $\mathbf{P}^{(n)} = \mathbf{P} + (\Delta q_P + n/D)\hat{z}$ satellite reflections around the substrate primary reflection, **P**, the effective and hybrid satellites would be extra features that also depends on the azimuthal sample position, and they are visible near the substrate effective reflections, $\mathbf{P}^* = \mathbf{S} + \mathbf{C}$. Instead of normal secondary and coupling reflections from a crystalline lattice, the effective satellites have these reflections given by satellite reflections, $\mathbf{S}^{(s)} = \mathbf{S} + (\Delta q_S + s/D)\hat{z}$ and $\mathbf{C}^{(c)} = \mathbf{C} + (\Delta q_C + c/D)\hat{z}$. Then,

$$P^{*(s+c)} = \mathbf{S}^{(s)} + \mathbf{C}^{(c)} = \mathbf{P} + [\Delta q_S + \Delta q_C + (s+c)/D]\hat{z}, \quad (1)$$

are the diffraction vectors of the effective satellites. Their excitement condition require that both vectors, $\mathbf{P}^{*(s+c)}$ and $\mathbf{S}^{(s)}$, fulfil simultaneously the diffraction condition. In other words, both vectors must be touching the surface of the Ewald sphere at the same time in order to excite an effective satellite. It will assure that the $\mathbf{C}^{(c)}$ reflections, the satellite-coupling reflections, are under diffraction condition to couple the beam scattered by the $\mathbf{S}^{(s)}$ reflections, the satellite-secondary reflections.

The ω and ϕ angles for exciting an effective satellite are easily determined by assuming that the surface-normal direction is aligned with the substrate primary reflection. With such simplification, the ω incidence angle for the effective satellites will be given by

$$\sin\omega = \lambda|\mathbf{P}^{*(s+c)}|/2, \quad (2)$$

and the ϕ angle by Ref. [2]

$$\cos(\phi - \alpha) = \frac{\lambda|\mathbf{S}^{(s)}|/2 - \sin\omega\cos\gamma}{\cos\omega\sin\gamma}, \quad (3)$$

where γ and α are the polar and azimuthal angles describing the $\mathbf{S}^{(s)}$ vectors in the $\hat{x}$, $\hat{y}$, and $\hat{z}$ orthogonal system of unit vectors. $\hat{x}$ and $\hat{y}$ lies in the sample surface plane as shown in Fig. 1.

Since $\Delta q_P = \Delta q_S + \Delta q_C$, the effective satellites, $\mathbf{P}^{*(s+c)}$, will have the same ω angle of the normal satellite, $\mathbf{P}^{(n)}$, where $n = s + c$. It implies that the SL_n^* may be formed by contributions from a set of different $\mathbf{S}^{(s)} + \mathbf{C}^{(c)}$ detour paths, those that have the sum $\mathbf{s} + \mathbf{c}$ equal to the effective satellite index, n. For simplicity, each possible detour path for a given effective index will be denoted hereafter by (s, c). However, even with the constraint of a common effective index, the (s, c) paths do not occur exactly at the same azimuthal angle. Their ϕ positions depend explicitly on the s index, as given by Eq. (3). These paths also differ from one to another by the δ angle in which the satellite-secondary beam, the beam diffracted by the $\mathbf{S}^{(s)}$ satellite-secondary reflection, crosses the interfaces of the layers. It can be calculated by

$$\cos(\pi/2 - \delta) = \lambda\mathbf{k}_S^{(s)}\cdot\hat{z}. \quad (4)$$

Hybrid satellites are mathematically described by the same equations presented above, Eqs. (1–4), when the satellite-secondary reflection, $\mathbf{S}^{(s)}$, is replaced by the substrate-secondary reflection itself, which gives

$$\mathbf{P}^{*(1/m+c)} = \mathbf{S} + \mathbf{C}^{(c)} = \mathbf{P} + [\Delta q_C + c/D]\hat{z}. \quad (5)$$

The superscript $1/m$ stands for $\Delta q_C = \Delta q_P/m$. Since $m \neq 1$, the ω angles for hybrid satellites do not coincide with

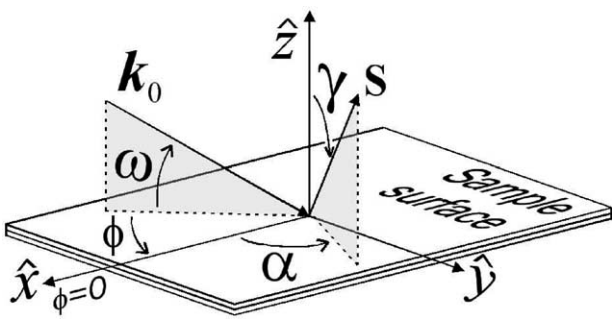

Fig. 1. Description of the incident beam wavevector, $\mathbf{k}_0$, and the diffraction vector, **S**, in a convenient orthogonal system of $\hat{x}$, $\hat{y}$ and $\hat{z}$ unit vectors where $\hat{z}$ is the surface normal direction.

the normal satellites. Their azimuthal position depend exclusively on the substrate parameters as shown by Eq. (3) for $\mathbf{S}$ instead of $\mathbf{S}^{(s)}$. There is also one more condition: δ in Eq. (4) must be positive, otherwise the secondary beam generated at the substrate lattice will not reach the superlattice that is laying at the top.

Although, Eqs. (2) and (3) allow a good understanding on the positioning of effective and hybrid satellites, they are difficult to handle for practical calculation. A very simple and general approach, not limited to the condition $\mathbf{P}\|\hat{z}$, can be obtained from the Bragg-cone equations in the reciprocal-space. For the secondary and coupling reflections [1],

$$\mathbf{k}_0\cdot\mathbf{S}^{(s)} = -\mathbf{S}^{(s)}\cdot\mathbf{S}^{(s)}/2 \tag{6a}$$

and

$$\mathbf{k}_S\cdot\mathbf{C}^{(c)} = -\mathbf{C}^{(c)}\cdot\mathbf{C}^{(c)}/2 \Rightarrow \mathbf{k}_0\cdot\mathbf{C}^{(c)} = -\mathbf{C}^{(c)}\cdot\mathbf{C}^{(c)}/2 - \mathbf{C}^{(c)}\cdot\mathbf{S}^{(s)}. \tag{6b}$$

Since the satellite reflections are close to the substrate reflections, the wavevector of the incident beam can be written relatively to the ω_0 and ϕ_0 positions of the chosen n-BD, then,

$$\mathbf{k}_0 \approx \mathbf{k}_{0\_sub} + \Delta\omega\mathbf{k}_\omega + \Delta\phi\mathbf{k}_\phi, \tag{7}$$

where

$$\mathbf{k}_{0\_sub} = -\lambda^{-1}(\cos\omega_0\cos\phi_0\hat{x} + \cos\omega_0\sin\phi_0\hat{y} + \sin\omega_0\hat{z}),$$

$$\mathbf{k}_\omega = -\lambda^{-1}(-\sin\omega_0\cos\phi_0\hat{x} - \sin\omega_0\sin\phi_0\hat{y} + \cos\omega_0\hat{z}),$$

$$\mathbf{k}_\phi = -\lambda^{-1}(-\cos\omega_0\sin\phi_0\hat{x} + \cos\omega_0\cos\phi_0\hat{y}),$$

$\Delta\omega = \omega - \omega_0$ and $\Delta\phi = \phi - \phi_0$. By replacing $\mathbf{k}_0$, from Eq. (7), into Eqs. (6a) and (6b), $\Delta\omega$ and $\Delta\phi$ are determined by solving the following trivial system of linear equations

$$\begin{bmatrix} a_{11} & a_{12} \\ a_{21} & a_{22} \end{bmatrix}\begin{bmatrix} \Delta\omega \\ \Delta\phi \end{bmatrix} = \begin{bmatrix} b_1 \\ b_2 \end{bmatrix}, \tag{8}$$

where $a_{11} = \mathbf{k}_\omega\cdot\mathbf{S}^{(s)}$, $a_{12} = \mathbf{k}_\phi\cdot\mathbf{S}^{(s)}$, $b_1 = -(\mathbf{S}^{(s)}/2 + \mathbf{k}_{0\_sub})\mathbf{S}^{(s)}$, $a_{21} = \mathbf{k}\omega\cdot\mathbf{C}^{(c)}$, $a_{22} = \mathbf{k}_\phi\cdot\mathbf{C}^{(c)}$, and $b_2 = -(\mathbf{C}^{(c)}/2 + \mathbf{S}^{(s)} + \mathbf{k}_{0\_sub})\cdot\mathbf{C}^{(c)}$. When $\mathbf{S}$ is used instead of $\mathbf{S}^{(s)}$, the $\Delta\omega$ and $\Delta\phi$ of the hybrid satellites are obtained. Moreover, in-plane lattice mismatch, $(\Delta a/a)_\|$, between the substrate and the superlattice can also be taking into account by displacing the satellite reciprocal points according to

$$\mathbf{G}^{(n)} = \mathbf{G} + [\Delta q_G + n/D]\hat{z} - [\mathbf{G} - (\mathbf{G}\cdot\hat{z})\hat{z}](\Delta a/a)_\|, \tag{9}$$

where $\mathbf{G}$ stands for $\mathbf{S}$ or $\mathbf{C}$.

4. Experimental

The experiments were carried out at the X-ray diffraction topography beam line, ID19, of the European Synchrotron Radiation Facility (ESRF). The wavelength, λ, was set to 1.48663 Å by a double bounce Si 111 monochromator. At the sample position, $\approx$150 m from the source, the size of beam is limited by slits to about 0.1×0.1 mm^2, the beam divergences are negligible, and the plane of incidence is vertical.

A $10\times$[GaAs/AlAs]/GaAs (001) superlattice was used as a sample. It has been early characterized by high-resolution X-ray diffraction of the 002 reflection, and the relevant values of the structure are: $D = 1223(10)$ Å (superlattice period), $\Delta q_{002} = -0.545(12)\times10^{-3}$ Å^{-1} (longitudinal distance of the zeroth-order satellite from the 002 substrate reciprocal lattice point), $n_{GaAs}/n_{AlAs} = 395/469$ (number of monolayers in each layer), and $\langle a\rangle = 5.6621(2)$ Å (average superlattice parameter). For this sample, the $\hat{x}$ and $\hat{z}$ unit vectors of the convenience system of coordinates are taken along the [110] and [001] substrate directions, respectively.

5. Results and discussions

Fast investigation on effective and hybrid satellites can be carried out by choosing appropriated n-BD cases. In general, small secondary diffraction vectors, i.e. reflections of low indexes, imply in low sensitive to the in-plane mismatch as

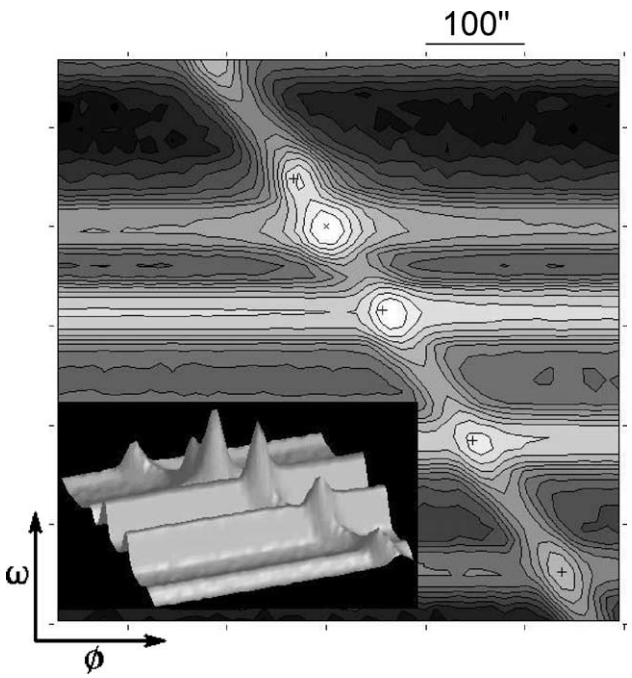

Fig. 2. Two-dimensional $\omega:\phi$ mapping around the $002^* = 1\bar{1}1 + \bar{1}11$ substrate 3-BD in the GaAs/AlAs superlattice. Its ω_0 (= 14.7562°) and ϕ_0 (= 5.3434°) position is given by the ' × ' mark. Besides the substrate and superlattice ordinary reflections, the mapped angular range also shown five effective satellites: SL0*, SL ± 1*, and SL ± 2*. The ' + ' marks give their expected positions. The contour map and the 3D surface (inset) show the log and root-square transformed intensity, respectively. Mesh resolution: 0.0032°. After Ref. [3].

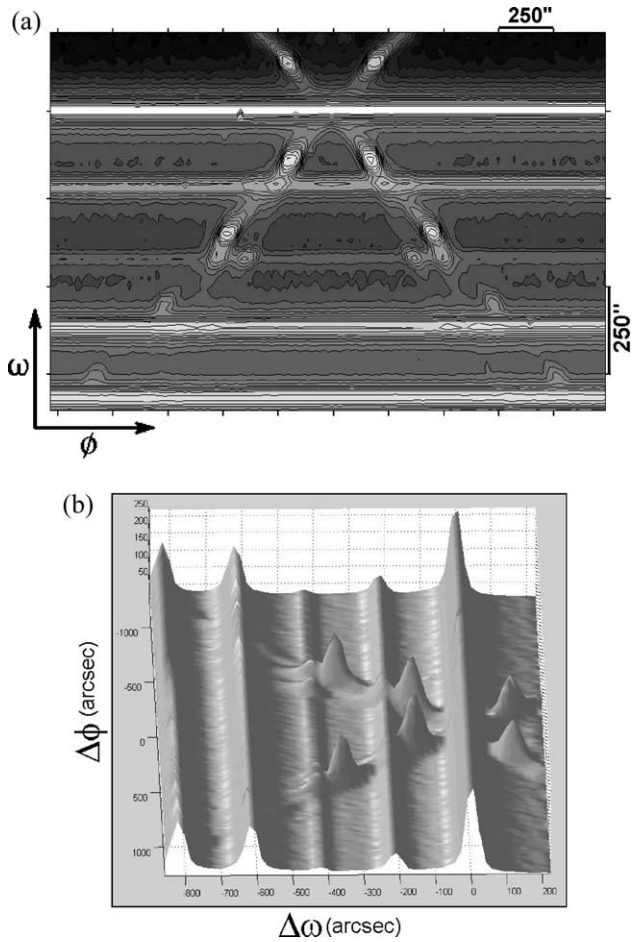

Fig. 3. Two-dimensional $\omega:\phi$ mapping around the 006/2$\bar{2}$4/$\bar{2}$24/2$\bar{2}$2/$\bar{2}$22 substrate 6-BD in the GaAs/AlAs superlattice. The contour map (a) and the 3D surface (b) show the log and root-square transformed intensity, respectively. Mesh resolution: 0.005°. The X is formed by the streaks of the 2$\bar{2}$4 and $\bar{2}$24 substrate-secondary reflections, whose positions are pointed out by hybrid satellites, i.e. the diffracted beam from these substrate reflections coupled by the structure of satellites around the $\bar{2}$22 and 2$\bar{2}$2 reflections. The center of the X is at $\omega_0 = 52.0815°$ and $\phi_0 = 0°$. More details on the features observed in this map are given in Fig. 4.

well as to the difference in ϕ of those effective satellites with a same ω angle. It also implies that the substrate secondary beam will not be able to reach the superlattice, preventing hybrid satellite reflections to occur. As can be seen in Fig. 2, the $\omega:\phi$ map of the $002^* = 1\bar{1}1 + \bar{1}11$ (P : 002, S : 1$\bar{1}$1, C : $\bar{1}$11) 3-BD clearly show that all (s,c) detour path with a same sum contributes to a single effective satellite peak, their ϕ positions coincide with the streak of the 1$\bar{1}$1 reflection, and no hybrid satellite is observed. To avoid similar redundant cases, this work investigates the structure of satellites at the 6-BD due to the 2$\bar{2}$4, 2$\bar{2}$2, $\bar{2}$24 and $\bar{2}$22 secondary reflections plus the 006 primary reflection. According to the notation $\mathbf{P}^* = \mathbf{S} + \mathbf{C}$, the 006^* can have simultaneous contributions from the following detour paths: (A) 2$\bar{2}$4 + $\bar{2}$22, (B) $\bar{2}$24 + 2$\bar{2}$2, (C) $\bar{2}$22 + 2$\bar{2}$4, and (D) 2$\bar{2}$2 + $\bar{2}$24. Only for A and B the secondary beams are scattered towards the superlattice. The $\omega:\phi$ map of this 6-BD is shown in Fig. 3. It embraces the 006 substrate reflection as well as the SL0, SL ± 1 and SL ± 2 satellite reflections, which appear as the straight horizontal lines, along the $\Delta\phi$ axis, in the intensity-contour plot (Fig. 3a). The streaks of the 2$\bar{2}$4 and $\bar{2}$24 substrate-secondary reflections are also visible forming the X. The intersection point over the 006 GaAs reflection is the exact condition of the 6-BD where all substrate-secondary reflections are excited. Its position correspond to $\omega_0 = 52.0815°$ and $\phi_0 = 0°$ if $\hat{x}$ is taken along the [110] direction. The position of these streaks are predicted by Eq. (6a), with $\mathbf{S}$ instead of $\mathbf{S}^{(s)}$, or in a first-order approximation by Eq. (8), which provides $\Delta\omega = (a_{12}/a_{11})\,\Delta\phi + b_1/a_{11}$. The azimuthal resolved peaks located over the streaks, in-between the satellites, are the $(1/3 + c)$ hybrid satellites where $\Delta q_C = \Delta q_{002} = \Delta q_{006}/3$. Those peaks at the top of the satellites are the effective ones, and in this case, it is possible to observe the split in ϕ of the (0,0) and $(-1, +1)$ effective satellites. A comparison between the experimental positions of the features in the $\omega:\phi$ map and their theoretical positions provide by Eq. (8) is given at Fig. 4.

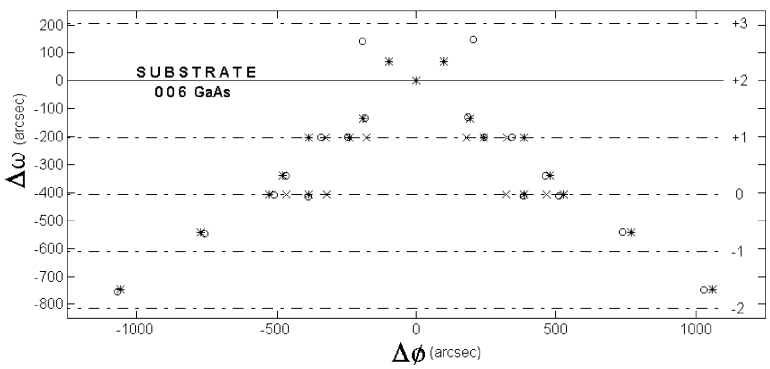

Fig. 4. A comparison between the experimental (○) and theoretical (∗) positions of the features in the $\omega:\phi$ map of the 6-BD shown in Fig. 3. The theoretical positions were given by Eq. (8). Besides the 006 substrate reflection (solid line) and the SL0, SL ± 1, SL ± 2, and SL ± 3 superlattice ordinary reflections (dashed lines), this map also shown hybrid and effective satellites. The $(1/3 + c)$ hybrid satellites, for $c = +1, 0, -1, -2$, and -3, are observed in-between the SL satellites from higher to lower ω angles, respectively. The effective ones are the peaks observed over the SL0 and SL + 1 satellites, corresponding to the (0,0), (+1, − 1), (+1,0) and (+2, − 1) detour paths. The × marks shown the expected shifts of the effective satellite peaks for $(\Delta a/a)_{\|} = 2.5 \times 10^{-4}$.

The most impressing features in the result shown in Fig. 3 are the intensities of the hybrid-satellite reflections, which are comparable to the intensities of the normal satellites. Then, even in conventional X-ray diffractometers they can be observed. Since those machines have a very poor azimuthal resolution, about 1°, rocking-curve characterization of superlattices can be jeopardized by such extra features if users are unwarned about them. On the other hand, effective satellites do not seriously compromise the conventional characterization since they can only be responsible to small changes in the intensities of the satellite reflections.

Synchrotron facilities in our days are almost available for any researcher, even in developing countries. Then, the hybrid and effective satellite phenomenon instead of being avoided, they should be better explored. At a first glance the interpretation of the $\omega : \phi$ maps seem to be complicated, but it is just because people are not used to them. The data collection is carried out with an open detector, which eliminates the need of any type of diffracted beam analyzer. Even thought two-dimensional reciprocal-space information can be withdrawn from a single map. The set of equations represented by Eq. (8) allows a direct correlation between the reciprocal space and the ω and ϕ positions of the features—note that this correlation is based on very simple dot products among reciprocal space vectors. The ϕ position of the effective satellites are extremely sensitive to the in-plane lattice mismatch of the superlattice. As simulated in Fig. 4, even for a tiny mismatch, $(\Delta a/a)_{\|}$, of 2.5×10^{-4} the shift in ϕ, $\Delta\phi$, is $62.3''$. In other words, $(\Delta a/a)_{\|} = 4 \times 10^{-6}\, \Delta\phi$ (arcsec). The azimuthal position of the hybrid satellites points out where is the streak of the substrate-secondary reflection, providing a reference to precisely determine the position of the effective satellites. Moreover, the ω angles of the hybrid satellites are mostly affected by the positioning of the satellite reciprocal points at the coupling reflection, i.e. they show how the substrate secondary beam see the structure of satellites around the coupling reflection.

Acknowledgements

This work has been greatly supported by the founding agency FAPEPS (Proc. No. 00/11554-7).

References

[1] S.L. Morelhão, E. Abramof, J. Appl. Crystallogr. 32 (1999) 871–877.
[2] H. Cole, F.W. Chambers, H.M. Dunn, Acta Crystallogr. 15 (1962) 138–144.
[3] S.L. Morelhão, L.H. Avanci, A.A. Quivy, E. Abramof, J. Appl. Crystallogr. 35 (2002) 69–74.